Sensors and Materials, Vol. 31, No. 9 (2019) 2917–2929
MYU Tokyo

S & M 1982

Impedimetric Biosensor for the Detection of Bacterial Lipopolysaccharide Based on Lectin-functionalized Gold Nanoparticle–Graphene Composites

Jianfang Qin, Hong Sun, Haoyong Hao, Lijuan Jia, Chenzhong Yao, Qianqian Wang, and Haiying Yang*

Department of Chemistry, Yuncheng University, Yuncheng 044300, P.R. China

(Received June 12, 2019; accepted July 31, 2019)

Keywords: bacterial lipopolysaccharide, impedimetric biosensor, graphene, electrodeposition of gold nanoparticles

We developed a simple impedimetric biosensor for the detection of bacterial lipopolysaccharide (LPS) based on lectin-functionalized gold nanoparticle (AuNP)–graphene (G) composites. The effects of AuNPs on G were investigated by comparison with the sensing surface in the absence of AuNPs. The results showed that the AuNPs formed a 3D micro/nanocomposite on G, which increased the electroactive area from 7.03×10^{-2} to 1.41×10^{-1} cm^2, and also increased the heterogeneous electron transfer rate, which can improve the sensitivity of the biosensor. Concanavalin A (Con A) lectin was used as a molecular recognition element because of its specific interaction toward the carbohydrate groups in LPS. The increase in electron transfer resistance was in a logarithmically direct proportion to the LPS concentration and lowered the detection limit to 600 pg/L. The fabricated biosensor achieved the detection of LPS with good sensitivity, acceptable reproducibility, and stability. This method may hold promise for potential applications in glycomic biosensing.

1. Introduction

Lipopolysaccharide (LPS, also known as bacterial endotoxin) is the main constituent of the outer membrane of gram-negative bacteria and mainly responsible for the integrity of the membrane and its low permeability, protecting the bacteria from chemical attacks by antibiotics.[1] Although LPS can have beneficial effects at low concentrations (for example, stimulating the immune response), it is toxic at high concentrations and can lead to septic shock and even death. The development of simple methods to detect LPS is therefore a challenging field of research.[2–4] Biosensors have emerged as one of the leading technologies for the detection of analytes of biological importance, either as stand-alone devices or as part of a biochip that can detect multiple analytes simultaneously.[5,6] Extensive efforts have been devoted to the design of novel biosensors for LPS or bacterial detection, including the employment of novel biological recognition molecules as well as highly sensitive detectors and detection techniques.[7–11]

*Corresponding author: e-mail: haiyingyang79@hotmail.com
https://doi.org/10.18494/SAM.2019.2421

ISSN 0914-4935

Electrochemical impedance spectroscopy (EIS) is frequently applied in the construction of label-free biosensors owing to its sensitivity and simple setup compared with other electrochemical sensing methods.[10–14] Graphene (G), a two-dimensional, single-layer sheet of sp^2 hybridized carbon atoms, has been widely explored in recent years because of its intriguing properties, such as large surface area, high electrical conductivity, good mechanical flexibility, chemical inertness, and low cost.[15–17] However, G tends to agglomerate or restack owing to strong π–π stacking and van der Waals interactions,[18] which hinder its future application. Introducing metal nanoparticles (NPs) was initially proposed to separate G sheets.[19,20]

Nowadays, it is considered that the dispersion of metal NPs on G sheets also potentially provides a new way of developing novel catalytic and optoelectronic materials. Gold nanoparticles (AuNPs) have recently been recognized as one of the most promising and efficient electrochemical and luminescence catalysts.[21,22] The incorporation of AuNPs and G always results in promising properties for sensor layers, especially the electrodeposition of AuNPs on the G surface because of their large surface to volume ratio and promising catalytic characteristics. We found that the *in situ* electrodeposition of NPs on a G and Nafion composite could provide an efficient biosensing surface for LPS detection with highly efficient electrochemical characteristics. Lectins can specifically bind to carbohydrate moieties and are particularly interesting candidates for use as molecular recognition elements because of the ease of their production and intrinsic stability. Several biosensors have been designed on the basis of the interactions between lectins and glycoproteins.[23–27] Concanavalin A (Con A) lectin is a carbohydrate-binding protein that specifically recognizes α-D-glucose and α-D-mannose groups and is one of the most commonly studied lectins that exist as a dimer below pH 5.5 and a tetramer between pHs 5.8 and 7.0. Furthermore, the biospecific interaction can prevent the chemical denaturation of the biomolecule without any chemical modification during the binding of lectin and carbohydrates. As gram-negative bacteria constantly shed LPS into their environment, it is an attractive target for detection.[1,4] Utilizing electrochemistry, we have incorporated this biological interaction into a functional sensor that can help inform clinicians.

The aim of this work was to develop a sensitive biosensor for LPS detection. As shown in Fig. 1, a label-free EIS biosensor was designed by using the significant effect of AuNPs on the improvement in electrochemical responses to fabricate a sensing layer as an amplification platform. Nafion was used here as a membrane matrix to improve the stability of the surface and prevent G from aggregating. The flowerlike AuNPs were electrodeposited onto the surface of the modified glassy carbon (GC) electrode with G and Nafion. Then, the recognition molecule Con A was immobilized by the self-assembly of 11-mercapto-1-undecanoic acid (MUA) using dithiothreitol (DTT) to block nonspecific interactions. Upon the binding of the target, the biosensor produces an increased EIS response that is directly proportional to the LPS concentration. Mannan is a polysaccharide with a strong affinity for Con A that is used to investigate the feasibility of the fabricated sensing layer. The characteristics and analytical performance of the biosensor are described.

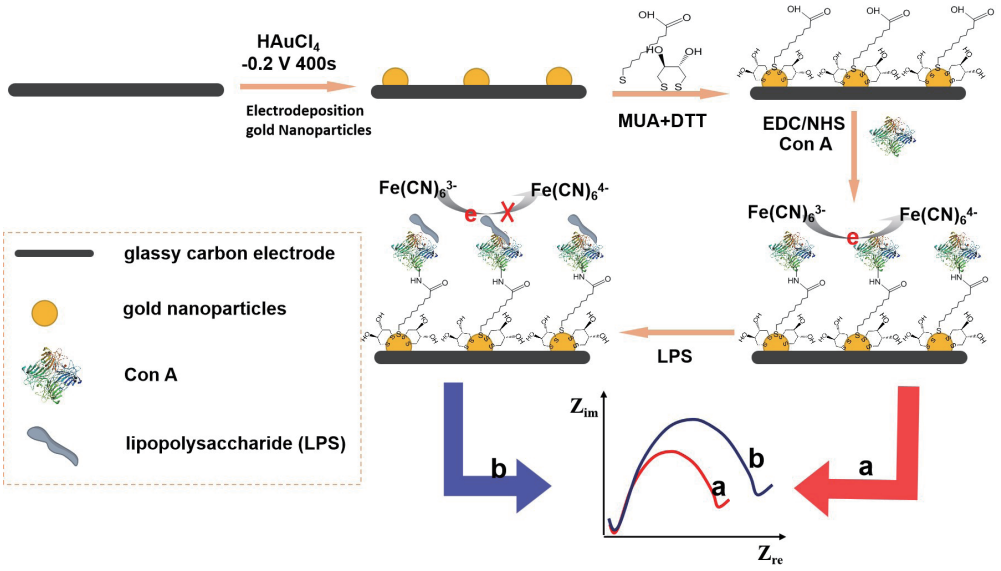

Fig. 1. (Color online) Schematic of impedimetric lectin-based biosensors for the determination of bacterial LPS.

2. Materials and Methods

2.1 Chemicals and materials

G was obtained from Nanjing Xianfeng Nanomaterials Technology Co., Ltd. (Nanjing, China). Con A from *Canavalia ensiformis*, type IV (Con A, *MW* = 104 kDa); bacterial LPS from *Escherichia coli* O55:B5; MUA; DTT; and all the carbohydrates used were obtained from Sigma-Aldrich (St. Louis, USA).

$HAuCl_4$ was supplied by Sinopharm Chemical Reagent Co., Ltd. (China). *N*-(3-dimethylaminopropyl)-*N*-ethylcarbodiimide hydrochloride (EDC), *N*-hydroxysuccinimide (NHS), and Nafion (5 wt%), in a mixture of low-molecular-weight aliphatic alcohols and water (contains 45% water), were purchased from Sigma Co., Ltd. (China). Potassium ferricyanide ($K_3[Fe(CN)_6]$), potassium ferrocyanide ($K_4[Fe(CN)_6]$), $MnCl_2$, $CaCl_2$, potassium chloride (KCl), and *N*,*N*-dimethylformamide (DMF) were obtained from Sinopharm Chemical Reagent Co., Ltd. (China). Bovine serum albumin (BSA) was obtained from Shanghai Sangon Biological Engineering Technology and Services Co., Ltd. (China). All reagents were used as supplied without further purification unless indicated.

Phosphate-buffered saline (PBS: 10 mM, pH 7.4, 10 mM Na_2HPO_4/NaH_2PO_4 and 100 mM KCl) was used as a Con A immobilization and washing buffer. PBS (10 mM) containing 1 mM $CaCl_2$ and 1 mM $MnCl_2$ was used as a binding buffer. All carbohydrate solutions were prepared using the binding buffer. Ultrapure water (18.2 MΩ cm) (Milli-Q, Millipore) was used in all experiments.

2.2 Apparatus and measurements

The morphology of the modified electrodes was characterized by scanning electron microscopy (SEM; Hitachi S-4800, Japan). A CHI-660 electrochemical workstation (Chenhua Instruments Co., Shanghai, China) was used for electrochemical measurements. All electrochemical experiments were performed using a conventional three-electrode system with a fabricated biosensor or a GC electrode (GCE) as the working electrode, a platinum wire as the counter electrode, and a Ag/AgCl (sat. KCl) electrode as the reference electrode. All potentials are reported with respect to the reference electrode.

2.3 Biosensor fabrication

Two milligrams of G was dispersed in 2 mL of DMF in an ultrasonicator for 2 h. Nafion (0.5 wt%) was added to the dispersion and then the solution was dispersed by ultrasonication for 2 h to form a homogeneous suspension. Finally, the dispersion solution containing G (1 g/L) and Nafion (0.5 wt%) at a ratio of 1:1 (v/v) was obtained.

Prior to use, the GCE was polished using an aqueous alumina slurry (0.3 and 0.05 μm) and then washed thoroughly with deionized water. Then, the electrode was washed thoroughly with Milli-Q water and dried in a nitrogen stream to obtain a clean surface.

A 5 μL suspension of G and Nafion was drop-cast on a clean GCE and allowed to dry at room temperature to obtain the G/Nafion/GCE. Next, AuNPs were electrodeposited onto the G/Nafion/GCE in a 3.0 mM $HAuCl_4$ and 0.5 M H_2SO_4 solution at a constant potential of −0.2 V for 400 s. The as-prepared electrode was denoted as AuNPs/G/Nafion/GCE. The obtained electrode was rinsed with water and dried for use in the following experiment.

A 10 μL mixture of 1 μM MUA and 10 μM DTT was dropped onto the pretreated AuNPs/G/Nafion/GCE surface. The electrode was kept in a refrigerator (4 °C) for 14 h to obtain MUA/AuNPs/G/Nafion/GCE. The modified electrode was activated in 100 μL of a freshly prepared solution containing 2 mg/mL EDC and 5 mg/mL NHS for 30 min to activate the carboxylic groups on MUA. The activated electrode was immersed in 100 μL of 1 g/L Con A solution for 1 h. Finally, 100 μL of 1% BSA was used to block the surface activate sites for 30 min. After each step, the electrode was rinsed thoroughly with washing buffer to remove adsorption components. The lectin-based biosensor (ConA/AuNPs/G/Nafion/GCE) was obtained and stored at 4 °C in PBS (pH 7.4).

2.4 Electrochemical measurements

The fabricated biosensor was immersed in 100 μL of 10 mM PBS containing different concentrations of mannan solutions for 60 min and then washed with 10 mM PBS. Electrochemical measurements were carried out in 5 mL of 10 mM PBS containing 5 mM $K_3[Fe(CN)_6]$ and 5 mM $K_4[Fe(CN)_6]$ at the equilibrium potential of $[Fe(CN)_6]^{3-/4-}$ with a 5 mV sinusoidal excitation amplitude.

The EIS spectra were recorded at 0.2 V (vs Ag/AgCl) within a frequency range from 100 kHz to 0.1 Hz with a sampling rate of 12 points per decade. A Randles equivalent circuit

[Fig. 3(a)] was chosen for the fitting of the measured EIS results. It consists of ohmic resistance (R_s), double-layer capacitance (C_{dl}), electron transfer resistance (R_{et}), and Warburg impedance (Z_w). R_s and Z_w represent the properties of the electrolyte solution, which affect the resistance and diffusion of the redox probe. C_{dl} and R_{et} depend on the dielectric or insulating features at the electrode−electrolyte interface and are affected by the change in resistance at the electrode interface. The impedance Z is reported as a Nyquist plot. The concentration of mannan was quantified by an increase in the electron transfer $\Delta R_{et} = R_{et,i} - R_{et,0}$, where $R_{et,0}$ and $R_{et,i}$ are the electron transfer resistances before and after incubation with carbohydrates, respectively.

Cyclic voltammetry (CV) was used to monitor the fabrication of the biosensor. Voltammograms were recorded from −0.2 to 0.6 V at a scan rate of 0.1 V/s. All electrochemical experiments were carried out at room temperature (25 ± 1 °C).

3. Results and Discussion

3.1 Characterization of the biosensor

The surface morphologies of (a) GCE, (b) G/Nafion/GCE, and (c) AuNPs/G/Nafion/GCE were determined by SEM, and the results are shown in Fig. 2. The surface of the bare GCE is smooth, whereas that of the G/Nafion/GCE is rougher and more crumpled than that of the GCE, indicating the presence of wrinkled G sheets. The images also show that the suspension

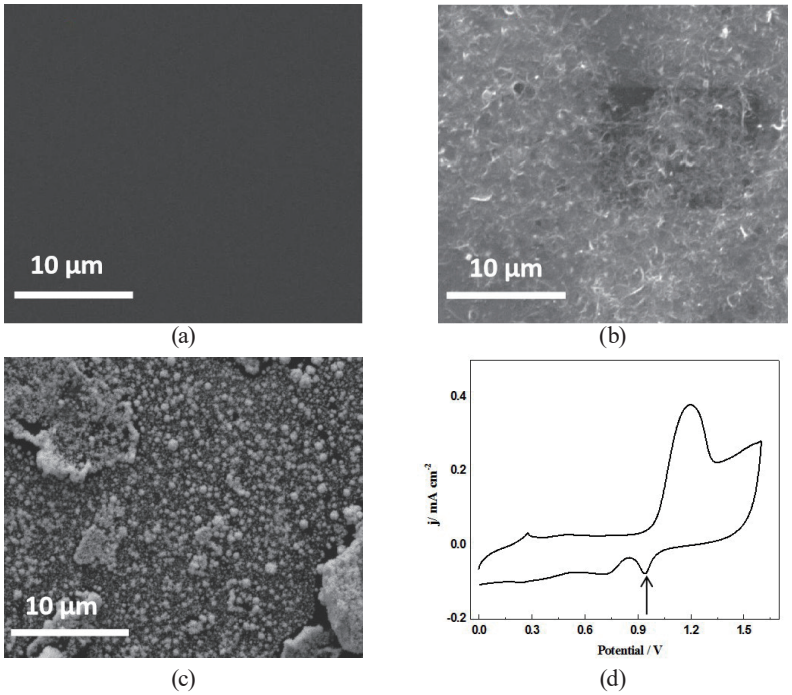

(a) (b) (c) (d)

Fig. 2. (Color online) Typical SEM images of different surfaces: (a) GCE, (b) G/Nafion/GCE, and (c) AuNPs/G/Nafion/GCE. (d) Cyclic voltammogram of the AuNPs/G/GCE in 0.5 M N_2-saturated H_2SO_4 solution at a scan rate of 10 mV/s. (Arrow shows the reduction of AuNPs).

of Nafion and G is uniformly coated on the GCE. AuNPs are shown in Fig. 2(c). Flowerlike AuNPs are seen as nearly uniform dispersed points on the G/Nafion/GCE surface.

The AuNPs were further characterized by recording the CV response of the AuNPs/G/Nafion/GCE in a 0.5 M N_2-saturated H_2SO_4 solution in the potential range of 0–1.6 V at a scan rate of 10 mV/s. Figure 2(d) shows the characteristic feature of the redox reaction of Au with two oxidation peaks at approximately +1.1 V (vs Ag/AgCl) corresponding to the formation of Au oxide and a reduction peak at approximately +0.9 V corresponding to the reduction of the same oxide.[27] These results further verify the formation of AuNPs on the G/Nafion/GCE.

3.2 Characterization of Con A-based biosensors by CV and EIS

To investigate the fabrication of the Con A-based biosensor, CV and EIS were performed after each step of the experiment in the solution of the electrochemical probe of ferri/ferrocyanide (Fig. 3). Electron transfer resistance (ΔR_{et}) was used as the signal because ΔR_{et} is the most direct and sensitive parameter that responds to the changes in the electrode interface. Mannan is a polysaccharide with a strong affinity for Con A, which is used here to further investigate its feasibility as the sensing layer.

An equivalent circuit [inset of Fig. 3(a)] was chosen to calculate the obtained impedance data. It includes the following components: the charge transfer resistance R_{et}, C_{dl} related to the interfacial double-layer capacity, the diffusion impedance Z_w, and the solution resistance R_s. The R_{et} of the electrode accounts for the diameter of the semicircle in the Nyquist plot. The R_{et} of the bare GCE exhibited a relatively low electron transfer resistance (224 Ω), indicating

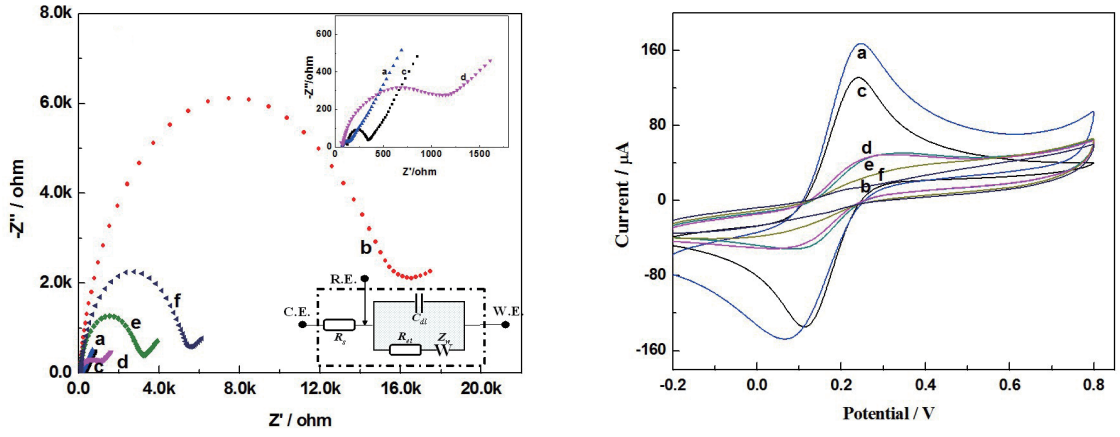

(a) (b)

Fig. 3. (Color online) Nyquist plots of the impedance spectra (a) and cyclic voltammograms (b) of different electrodes in each step. a, Bare GCE; b, G/Nafion/GCE; c, AuNPs/G/Nafion/GCE; d, Con A/AuNPs/G/Nafion/GCE; e, incubated with BSA; f, incubated with 0.05 nM mannan for 60 min. Inset: (a) Randles equivalent circuit used to model the impedance data in the presence of the redox couple (right-hand corner). The EIS measurements were carried out in 10 mM PBS (pH 7.4) containing 5 mM $K_3[Fe(CN)_6]$ and 5 mM $K_4[Fe(CN)_6]$ and 0.10 M KCl, while applying an amplitude of 5 mV in the frequency range of 0.1−100 kHz.

a very fast electron transfer. When G and Nafion were modified on the GCE surface, a large increase in charge transfer resistance (18520 Ω) was obtained. It is worth noting that the Nafion molecules obstructed the charge transfer and therefore contributed to the increase in semicircle diameter. After the AuNPs were electrodeposited onto the surface of the G/Nafion-modified GCE, R_{et} markedly decreased to 90 Ω, which demonstrated that AuNPs accelerate the electron transfer and would be beneficial for the improvement of the biosensor sensitivity.

The introduction of the mixed self-assembled monolayers (SAMs) of the MUA + DTT binary layer on the electrode and covalently coupled Con A resulted in the R_{et} increase from 90 to 1234 Ω. This is attributed to the insulating nature of the formed highly ordered and oriented SAM of MUA + DTT, which suppresses the penetration of redox species at the electrode surface.[10] Con A was immobilized by the carboxyl group of MUA by carbodiimide chemistry. Subsequently, after the functionalized electrode was blocked with BSA, R_{et} increased to 3266 Ω. This result, extracted from EIS measurements, is in good agreement with the results obtained by CV. These increases are mainly ascribed to the insulating properties of the proteins Con A and BSA, which prevent the redox species from accessing the electrode surface from the solution. After the biosensor binds with 0.05 nM mannan, R_{et} increases continuously, suggesting that G, AuNPs, and Con A have been successively assembled onto the GCE in sequence and that the as-designed electrochemical biosensor has been successfully fabricated.

3.3 Effect of the AuNPs electrodeposited on the biosensor

To illustrate the function of AuNPs in biosensor performance, the effective surface area of the electrodes could also be estimated on the basis of the Randles−Sevcik equation,[29,30]

$$I_{pc} = 2.69 \times 10^5 n^{3/2} A D^{1/2} C v^{1/2}, \quad (1)$$

where I_{pc} is the reduction peak current (A), n is the electron transfer number, A is the apparent electrode area (cm^2), D is the diffusion coefficient of $K_3[Fe(CN)_6]$ in the solution (cm^2/s), C is the $K_3[Fe(CN)_6]$ concentration (M), and v is the scan rate (V/s). By investigating the reduction in peak current with the scan rate, we calculate the average apparent electrode areas of G/Nafion/GCE and AuNPs/G/Nafion/GCE as 7.03×10^{-2} and 1.41×10^{-1} cm^2, respectively. In contrast to G/Nafion/GCE, the incorporated AuNP composite showed a larger active surface area, which may be attributed to its 3D network micro/nanostructure.[31] Notably, the electrodeposited AuNPs offered a larger active area than the stacked G sheets. The sufficient active area of the AuNPs/G/Nafion composite could result from the strong synergistic effects of the well-dispersed AuNPs and G.

It was also found that the anodic peak potential of AuNPs/G/Nafion/GCE shifted to a more positive value with increasing scan rate, whereas the cathodic peak potential shifted in the negative direction. Simultaneously, the peak current increased with the scan rate at higher sweep rates from 100 to 650 mV/s. The plots of the anodic and cathodic peak currents are proportional to the square root of the scan rate, showing a diffusion-controlled process (figure not shown). This result indicated that the rate of electrode reaction is mainly controlled by the

rate of redox species molecular diffusion from the solution to the modified electrode at a high scan rate, i.e., $K_4[Fe(CN)_6]$ and $K_3[Fe(CN)_6]$ are not or weakly adsorptive at the surface of the modified electrode.

Kinetic parameters for the reaction of $K_4[Fe(CN)_6]$ and $K_3[Fe(CN)_6]$ at the modified electrode can be measured from the potential difference between the oxidation and reduction peaks (ΔE_p) as a function of the scan rate.[32] As shown in Fig. 4, ΔE_p ranges from 0.16 to 0.24 mV and increases at a higher scan rate, indicative of the quasi-reversible kinetics in the system. Following Nicholson's working curve, the ΔE_p values can be converted into a dimensionless kinetic parameter ψ, which is directly proportional to the reciprocal of the square root of the scan rate, $v^{-1/2}$.

$$\psi = k^0 \left[\pi D n v F / (RT)\right]^{-1/2} \tag{2}$$

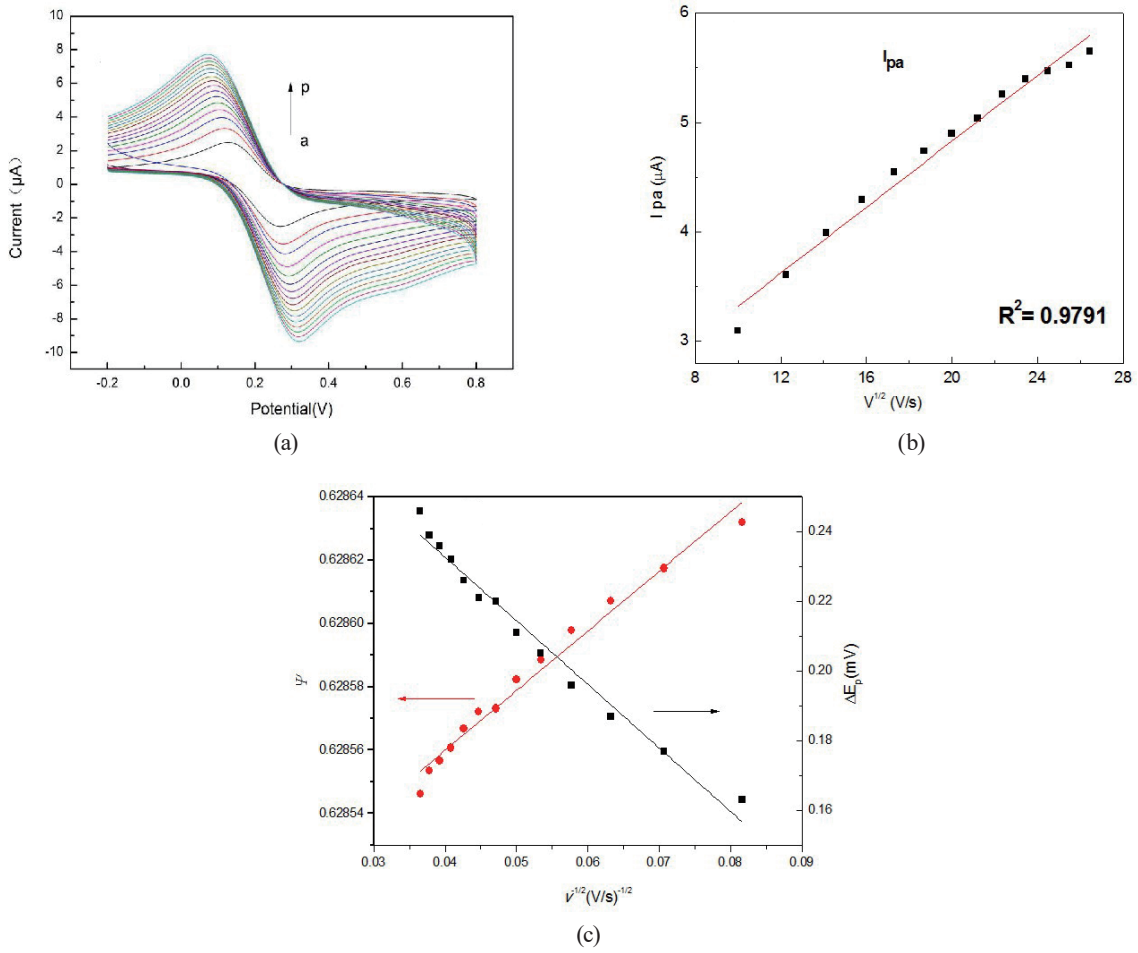

Fig. 4. (Color online) Electrochemistry at the AuNPs/G/Nafion/GCE. (a) Cyclic voltammograms of the modified electrode in 5 mM $K_4[Fe(CN)_6]/K_3[Fe(CN)_6]$ with 0.10 M KCl at different potential scan rates. (b) Plot of the anodic peak current ($i_{p,a}$) versus the square root of the potential scan rate ($v^{1/2}$). (c) Peak separation ΔE_p and Nicholson's kinetic parameter ψ versus the reciprocal of the square root of the potential scan rate ($v^{-1/2}$). A linear fit is used to determine k^0.

The standard heterogeneous electron transfer rate constant (k^0) can thus be determined from a linear fit to the $\psi - v^{-1/2}$ relationship (Fig. 4). From the slope according to the following equations, k^0 was obtained as approximately 4.33×10^{-5} s^{-1}.

$$k^0 = 2.18[D\beta nvF/(RT)]^{1/2} \exp[-(\beta^2 nF/RT)\cdot(E_{p,a} - E_{p,c})] \quad (3)$$

$$\Psi = (-0.6288 + 0.0021X)/(1 - 0.0017X) \quad (4)$$

$$X = n\Delta E_p(mV) \quad (5)$$

Therefore, it can be deduced that the composite of AuNPs/G/Nafion may provide not only an abundance of effective electron transfer pathways but also an accessible surface area for better self-assembly of MUA through the formation of the Au–S bond.[10,33–36] These could be beneficial for the high sensitivity of the biosensor in this work.

3.4 Optimization of the experimental parameters

Experimental parameters, including the Con A concentration during fabrication and the volume ratio in a mixed suspension of G and Nafion, were optimized. As expected, the Con A concentration directly affects the surface coverage of the recognition element on the modified electrode and further affects the sensitivity of the biosensor. Figure 5(a) shows the dependence of ΔR_{et} on the Con A concentration. After binding with 0.05 and 0.5 nM mannan, ΔR_{et} increases with the Con A concentration and then reaches a peak at approximately 1.0 g/L. The peak is attributed to the saturation of the surface coverage of Con A on the modified electrode. Therefore, to minimize the consumption of Con A, 1.0 g/L Con A was used in the following experiments.

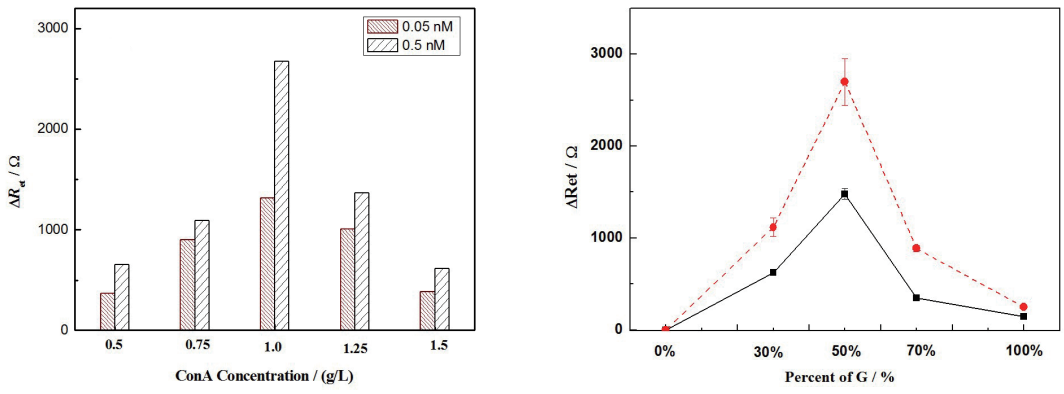

Fig. 5. (Color online) Effects of (a) Con A concentration and (b) G percentage in the composite on the response after biosensor incorporation with 0.05 and 0.5 nM mannan (n = 3).

The volume ratio of G in a mixture suspension of G and Nafion is important for the performance of the biosensor. Hence, the effect of the volume ratio of G in the mixture suspension on the behavior of the working electrode was investigated. After the biosensor was bound with 0.05 and 0.5 nM mannan, ΔR_{et} was measured at a series of volume ratios of G from 0 to 50%. ΔR_{et} began to increase with the volume ratio of G. However, from 50 to 100%, R_{et} decreased, as shown in Fig. 5B. Given the electron transfer resistance and the specific binding affinity of mannan and Con A, a 50% volume ratio of G was selected for further experiments.

3.5 Analytical performance of Con A-based biosensors

Under the optimized conditions, the behavior of the biosensor was quantitatively assessed by measuring the dependence of ΔR_{et} on the LPS concentration. Figure 6 shows the Nyquist plots of the faradaic impedance spectra for the biosensor with different LPS concentrations. Figure 6(b) shows the logarithmic relationship between ΔR_{et} and the LSP concentration in the range of 1.0×10^{-9} to 1.0×10^{-6} g/L. The regression equation was $\Delta R_{et} = 1761\log C + 16108$ (C is in units of g/L) with a regression coefficient of 0.9890. The detection limit was calculated to be 6.0 × 10 pg/L on the basis of a signal-to-noise ratio of 3.

The reproducibility of the biosensors was evaluated by assaying five biosensors prepared separately by the same fabrication procedure. The acceptable reproducibility was obtained with a relative standard deviation (*RSD*) of 4.6%. The biosensor for binding mannan was also investigated. The *RSD*s for five biosensors prepared separately with the same fabrication procedure were 4.6 and 4.2% at mannan concentrations of 0.05 and 0.5 nM, respectively. The results suggest that an acceptable reproducibility was obtained in this work.

Furthermore, the storage stability of the proposed biosensor was also studied. EIS was carried out to measure the response of the biosensor to 0.5 nM mannan. The biosensor lost approximately 9.5 and 12.4% of its original response after 10 and 20 days, respectively, indicating acceptable stability. This might be because G and Au nanocomposites, which

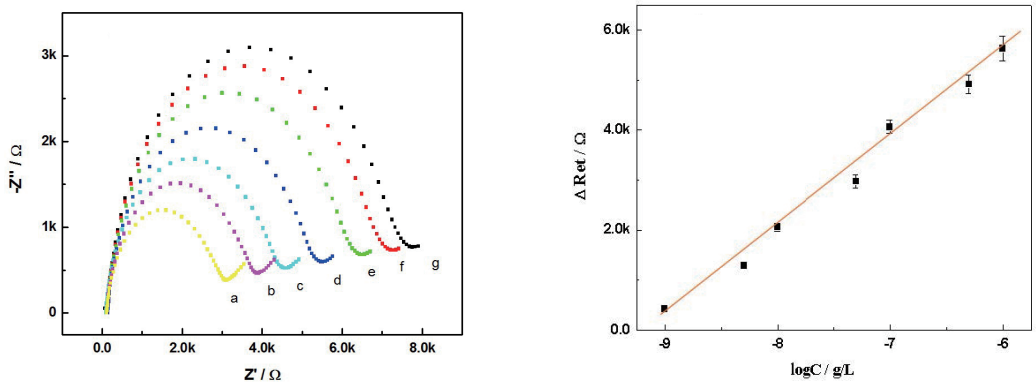

(a) (b)

Fig. 6. (Color online) (a) Nyquist plots of impedance spectra of the Con A/AuNPs/G/Nafion/GCE interacted with LPS at different concentrations: a, 1.0×10^{-9}; b, 5.0×10^{-9}; c, 1.0×10^{-8}; d, 5.0×10^{-8}; e, 1.0×10^{-7}; f, 5.0×10^{-7}; g, 1.0×10^{-6} g/L. (b) Linear relationship between ΔR_{et} and LPS concentration.

possess a large effective surface area and a strong electrical conductivity, offer a favorable immobilization platform for molecular recognition elements.

Various carbohydrates were tested to evaluate the selectivity of the biosensor, that is, the specific binding of the biosensor with mannan and the nonspecific binding with D-galactose, sucrose, rhamnose, fucose, and cellobiose. The results of electrochemical measurements described in Sect. 2.4 are shown in Fig. 7. The measured $\Delta R_{et}/R_{et,0}$ values were 4.03 for mannan and only 0.06–0.22 for the other carbohydrates. The difference in $\Delta R_{et}/R_{et,0}$ value clearly indicated the binding affinities of Con A toward the target. Under neutral conditions, each subunit of Con A contains three binding sites. One is for calcium and manganese cations to activate the binding site of the protein for carbohydrates, one is for hydrophobic recognition, and one is specific for the r-mannose or D-glucose residue, which has an affinity similar to that between lectin and the carbohydrate ligand. Thus, this might be because the binding activity of Con A extends only toward the vicinal, equatorial hydroxyl groups present in the carbohydrate stereochemistry of 3–OH and 4–OH carbohydrates such as mannan, while the other carbohydrates used as the control do not have groups such as these.[10,25–27] Hence, Con A rarely binds with control carbohydrates because it has axial 4–OH, thus possessing a fundamentally different stereochemistry.

To estimate the binding strength between lectin and mannan, the binding constant was calculated. Assuming that the interaction between lectin and mannan was in accordance with the Langmuir isotherm, binding strengths at all binding sites were the same. The binding constant (K) of the immobilized Con A with mannan was determined by the proposed EIS method[37] to be 5.9×10^9 M^{-1} from the plot of $C/\Delta R_{et}$ as a function of C representing a Langmuir adsorption isotherm (where C is the mannan concentration). This value is consistent with 5.3×10^9 M^{-1} obtained by SPR for yeast mannan and Con A,[38] and is slightly lower than 5.2×10^{10} M^{-1} obtained by ECL for Con A immobilized on SWCNT.[9] This large K suggests that the binding strength between mannan and the surface-confined Con A is significantly large.[9,10]

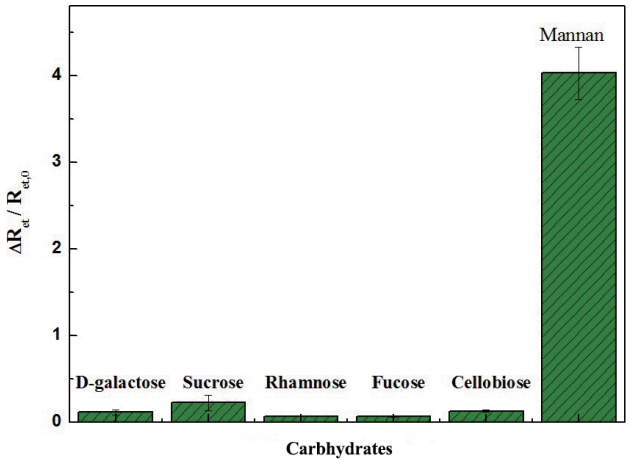

Fig. 7. (Color online) EIS responses of the biosensor to different carbohydrates at a concentration of 0.5 nM for an incubation time of 60 min. The EIS measurement conditions were the same as those in Fig. 2.

4. Conclusion

An impedimetric Con A-based biosensor was developed to detect bacterial LPS. The electrochemically deposited AuNPs that formed a 3D micro/nanocomposite increased not only the electrocatalytic surface area and the number of immobilized molecular recognition elements but also the heterogeneous electron transfer rate, which was ascribed to the improved sensitivity of the fabricated sensor. This method may also hold promise for potential applications in glycomic biosensing and DNA nanostructure framework construction.

Financial Interest

The authors declare no financial interest.

Acknowledgments

The authors acknowledge the financial support of this work by the National Natural Science Foundation of China (No. 21576230) and the Natural Science Foundation of Shanxi Province for Outstanding Young Scholars (No. 201701D211004).

References

1 B. Beutler and E. T. Rietschel: Nat. Rev. Immunol. **3** (2003) 169. https://doi.org/10.1038/nri1004
2 V. Ganesh, K. Bodewits, S. J. Bartholdson, D. Natale, D. J. Campopiano, and J. C. Mareque-Rivas: Angew. Chem. Int. Ed. **48** (2009) 356. https://doi.org/10.1002/anie.200804168
3 B. S. Park, D. H. Song, H. M. Kim, B. S. Choi, H. Lee, and J. O. Lee: Nature **458** (2009) 1191. https://doi.org/10.1038/nature07830
4 J. Wu, A. Zawistowski, M. Ehrmann, T. Yi, and C. Schmuck: J. Am. Chem. Soc. **133** (2011) 9720. https://doi.org:10.1021/ja204013u
5 M. Labib, E. H. Sargent, and S. O. Kelley: Chem. Rev. **116** (2016) 9001. https://doi.org/9001.10.1021/acs.chemrev.6b00220
6 Z. Meng, R. M. Stolz, L. Mendecki, and K. A. Mirica: Chem. Rev. **119** (2019) 478. https://doi.org/10.1021/acs.chemrev.8b00311
7 G. Acharya, C. L. Chang, and C. Savran: J. Am. Chem. Soc. **128** (2006) 3862. https://doi.org/10.1021/ja0574901
8 M. A. Seia, S. V. Pereira, C. A. Fontán, I. E. De Vito, G. A. Messina, and J. Raba: Sens. Actuators, B **168** (2012) 297. https://doi.org/10.1016/j.snb.2012.04.026
9 H. Yang, Y. Wang, H. Qi, Q. Gao, and C. Zhang: Biosens. Bioelectron. **35** (2012) 376. https://doi.org/10.1016/j.bios.2012.03.021
10 H. Yang, H. Zhou, H. Hao, Q. Gong, and K. Nie: Sens. Actuators, B **229** (2016) 297. https://doi.org/10.1016/j.snb.2015.08.034
11 P. Koedrith, T. Thasiphu, K. Tuitemwong, R. Boonprasert, and P. Tuitemwong: Sens. Mater. **26** (2014) 711. https://myukk.org/SM2017/sm_pdf/ SM1036.pdf
12 R. Mayall, M. Renaud−Young, N. Chan, and V. Birss: Biosens. Bioelectron. **87** (2012) 794. https://doi.org/10.1016/j.bios.2016.09.009
13 M. Zhang, Q. Zhai, L. Wan, L. Chen, Y. Peng, C. Deng, J. Xiang, and J. Yan: Anal. Chem. **90** (2018) 7422. https://doi.org/10.1021/acs.analchem.8b00884
14 C. Li, D. Chen, Y. Wang, X. Lai, J. Peng, X. Wang, K. Zhang, and Y. Cao: Sensors **19** (2019) 1304. https://doi.org/10.3390/s19061304
15 S. Stankovich, D. A. Dikin, G. H. Dommett, K. M. Kohlhaas, E. J. Zimney, E. A. Stach, R. D. Piner, S. T. Nguyen, and R. S. Ruoff: Nature **442** (2006) 282. https://doi.org/10.1038/nature04969
16 A. Fasolino, J. Los, and M. I. Katsnelson: Nat. Mater. **6** (2007) 858. https://doi.org/10.1038/nmat2011

17 M. D. Stoller, S. Park, Y. Zhu, J. An, and R. S. Ruoff: Nano Lett. **8** (2008) 3498. https://doi:10.1021/nl802558y
18 H. Hu, X. Wang, J. Wang, L. Wan, F. Liu, H. Zheng, R. Chen, and C. Xu: Chem. Phys. Lett. **484** (2010) 247. https://doi.org/10.1016/j.cplett.2009.11.024
19 Y. Si and E. T. Samulski: Chem. Mater. **20** (2008) 6792. https://doi.org/10.1021/cm801356a
20 R. Pasricha, S. Gupta, and A. K. Srivastava: Small **5** (2009) 2253. https://doi.org/10.1002/smll.200900726
21 Y. H. Lu, M. Zhou, C. Zhang, and Y. P. Feng: J. Phys. Chem. C **113** (2009) 20156. https://doi.org/10.1021/jp908829m
22 C. Guo, J. Wang, X. Chen, Y. Li, L. Wu, J. Zhang, and C. Tao: Sensors **19** (2019) 40. https://doi.org/10.3390/s19010040
23 N. Sharon and H. Lis: Glycobiology **14** (2004) 53. https://doi.org/10.1093/glycob/cwh122
24 L. N. Cella, W. Chen, N. V. Myung, and A. Mulchandani: J. Am. Chem. Soc. **132** (2010) 5024. https://doi.org/10.1021/ja100503b
25 F. Hu, S. Chen, C. Wang, R. Yuan, Y. Xiang, and C. Wang: Biosens. Bioelectron. **34** (2012) 202. https://doi.org/10.1016/j.bios.2012.02.003
26 Y. Wang, Z. Ye, and Y. Ying: Sensors **12** (2012) 3449. https://doi.org/10.3390/s120303449
27 F. Ma, A. Rehman, M. Sims, and X. Zeng: Anal. Chem. **87** (2015) 4385. https://doi.org/10.1021/acs.analchem.5b00165
28 Y. Hu, J. Jin, P. Wu, H. Zhang, and C. Cai: Electrochim. Acta **56** (2010) 491. https://doi.org/10.1016/j.electacta.2010.09.021
29 W. Sun, X. Qi, Y. Chen, S. Liu, and H. Gao: Talanta **87** (2011) 106. https://doi.org/10.1016/j.talanta.2011.09.047
30 S. Rengaraj, A. Cruz−Izquierdo, J. L. Scott, and M. Di Lorenzo: Sens. Actuators, B **265** (2018) 50. https://doi.org/10.1016/j.snb.2018.03.020
31 C. E. Zou, B. Yang, D. Bin, J. Wang, S. Li, P. Yang, C. Wang, Y. Shiraishi, and Y. Du: J Colloid Interface Sci. **488** (2017) 135. https://doi.org/10.1016/j.jcis.2016.10.088
32 W. Li, C. Tan, M. A. Lowe, H. D. Abruna, and D. C. Ralph: ACS Nano **5** (2011) 2264. https://doi.org/10.1021/nn103537q
33 L. Zhao, C. Li, H. Qi, Q. Gao, and C. Zhang: Sens. Actuators, B **235** (2016) 575. https://doi.org/10.1016/j.snb.2016.05.136
34 Q. L. Wang, H. F. Cui, X. Song, S. F. Fan, L. L. Chen, M. M. Li, and Z. Y. Li: Sens. Actuators, B **260** (2018) 48. https://doi.org/10.1016/j.snb.2017.12.105
35 Y. Qi, J. He, F. R. Xiu, X. Yu, Y. Li, Y. Lu, X. Gao, Z. Song, and B. Li: Spectrosc. Spectrochim. Acta A **216** (2019) 310. https://doi.org/10.1016/ j.saa.2019.03.073
36 Y. Qi, J. He, F. R. Xiu, X. Yu, X. Gao, Y. Li, Y. Lu, and Z. Song: Microchem. J. **147** (2019) 789. https://doi.org/10.1016/j.microc.2019.03.095
37 S. Szunerits, J. Niedziółka-Jönsson, R. Boukherroub, P. Woisel, J. S. Baumann, and A. Siriwardena: Anal. Chem. **82** (2010) 8203. https://doi.org/10.1021/ac1016387
38 J. Masárová, E. S. Dey, J. Carlsson, and B. Danielsson: J. Biochem. Bioph. Methods **60** (2004) 163. https://doi.org/10.1016/j.jbbm.2004.05.005